UDC 539.3

N. D. Vaysfeld, Z. Yu. Zhuravlova✉

EXACT SOLUTION TO THE POROELASTICITY PROBLEM FOR A MULTILAYERED RECTANGULAR DOMAIN

The poroelastic stress state of a layered rectangular domain is considered in terms of a boundary value problem of poroelasticity theory. The proposed analytical solution method makes it possible to derive an exact solution to the problem in the case of perfect contact between layers. The obtained explicit-form formulas for the determination of stresses, displacements, and pore pressure allow for performing broad computational analysis which demonstrates the dependence of the stress state on the poroelastic properties of the materials. This approach can be extended to the case where conditions of weak or stiff contact are imposed on the layer interfaces.

Key words: *poroelastic multilayered rectangular domain, integral transform, matrix differential calculus, exact solution.*

Poroelastic multilayered rectangular domains can serve models of a cross-section of the Earth's crust or an area with multiple layers of soil, rock, or water. The layers of materials (such as asphalt, concrete, and gravel) are used in the pavement industry [22] or foundation and other structures. A rectangle represents a bounded area, so it is necessary to consider not only the conditions between layers, but also boundary conditions on the edges of rectangle. Such a formulation of the problem often leads to mathematical difficulties in its solution. This explains the rather large number of approximate numerical methods for studying such domains.

As an example, the fast powerful numerical scheme to calculate poroelastic solutions for excess pore pressure and displacements in a multilayered half-space is presented in [27]. Vertical vibrations of a group of flexible strip foundations on multilayered transversely isotropic poroelastic soils are presented in [19], and the dynamic interaction problem is studied by employing a variational approach based on the discretization of the strip-soil contact region.

The development of analytical methods for solving problems for rectangular regions is often based on the use of the results of numerical analysis. An analytical layer-element solution to nonaxisymmetric consolidation of multilayered poroelastic materials with anisotropic permeability and compressible constituents is presented in [11], but the actual solutions in the physical domain are acquired by applying numerical quadrature schemes for the inversion of the Laplace – Hankel transform. Dynamic impedance functions for multiple strip footings bonded to the surface of a multilayered transversely isotropic poroelastic half-plane are presented in [20], where the dynamic interaction problem is investigated by using the exact stiffness matrix method and a discretization technique. The dynamic response of a transversely isotropic and multilayered poroelastic medium over an impermeable rigid base due to a surface strip load moving with constant speed is investigated in [16], the semi-analytical solution is derived by using Fourier series, potential-function method and position method along with the continuity conditions on the layer interface.

The use of analytic solution methods towards the problems for a finite rectangular region is associated with significant mathematical difficulties and is therefore accompanied by a radical simplification of the problems statements. If, for example, the problems are considered in reduced dimensional formulations, then some boundary conditions can be neglected. This explains

✉ z.zhuravlova@onu.edu.ua

DOI: 10.15407/mmpmf2024.67.3-4.118-131

the large number of papers devoted to the study of poroelastic infinite or semi-infinite regions, such as half-space, half-plane, slab, media, etc. The investigation of the dynamic behavior of layered transversely isotropic poroelastic media subjected to rectangular harmonic loads is provided in [9] by means of integral transform techniques and extended precise integration method. Vertical vibration of a rigid disk embedded in a multilayered poroelastic medium is considered in [23]. An analytical solution is constructed by using the Fourier and Hankel integral transforms, and Green's functions. The dynamic responses of an anisotropic multilayered poroelastic half-space to a point load or a fluid source are studied in [26] based on Stroh formalism and Fourier transforms. An osteon is idealized in [13] as a hollow two-dimensional poroelastic multilayered slab model subjected to cyclic loading. Based on poroelastic theory, the analytical solutions of interstitial fluid pressure and seepage velocity in lacunar-canalicular pores are obtained there. The response of multilayered transversely isotropic poroelastic media under vertical rectangular moving loads is investigated in [10] by utilizing the extended precise integration method. The dynamic response of multiple flexible strip foundations resting on a multilayered poroelastic half-plane subjected to time-harmonic vertical loading is studied in [18] with the help of the application of Lagrange's equations of motion. The problem of the two-dimensional plane strain deformation of a multilayered poroelastic half-space by surface loads is formulated in [21]. The formal solution is obtained by using Fourier – Laplace transforms and generalized Thomson – Haskell matrix method.

The elasticity and thermoelasticity problems for multilayered bodies are extensively studied in mechanics of coupled fields [1]. An analytic-numerical method for the determination of one-dimensional static thermoelastic state of plane multilayer structures with arbitrary type of temperature dependence of the physical and mechanical characteristics of materials of their components is proposed in [5]. An approach for solving plane axisymmetric problems of elasticity and thermoelasticity for multilayer hollow cylinders with per-layer properties having arbitrary distribution profiles within the radial coordinate is presented in [23]. Based on static and quasistatic methods of measurements with regard for the initial stress in the material the analysis of the existing methods for the determination of physical constants of porous media saturated with liquids is provided in [4]. The methods of thermodynamics of irreversible processes and functional analysis are applied in [17] in order to formulate the mathematical model of thermoelastic solid body taking into account the structural heterogeneity of the body material and geometric irregularity of its surface. Under the action of a thermal dipole, the Green's functions of the problems of stationary heat conductivity and thermoelasticity are constructed in [2] for plane deformation of a semi-infinite body with a free, rigidly, smoothly or flexibly clamped boundary on which zero temperature is maintained. Contact interaction between two elastic semi-infinite bodies in the presence of a real gas in interface gaps, which are caused by a periodic array of grooves on the surface of one of the bodies, is modeled in [3]. On the base of Helmholtz potentials properties the representations for the displacements in 3D elastic bimaterial with the time-harmonic vibrating cracks, which satisfy identically the perfect contact conditions on the interface, are obtained in [6]. Methods for solving two-dimensional boundary value problems of mathematical cracks theory for isotropic bodies are considered in [7].

A different approach to solving poroelasticity problems is proposed by the authors in the present paper.

1. Statement of the problem. We consider a poroelastic multilayered rectangle $0 < x < a$, $0 < y < 1$ (Fig. 1) within the framework of the Biot's model [12]. The rectangle consists of N layers $a_{i-1} < x < a_i$, $i = 1,\ldots,N$, where $a_0 = 0$, $a_N = a$.

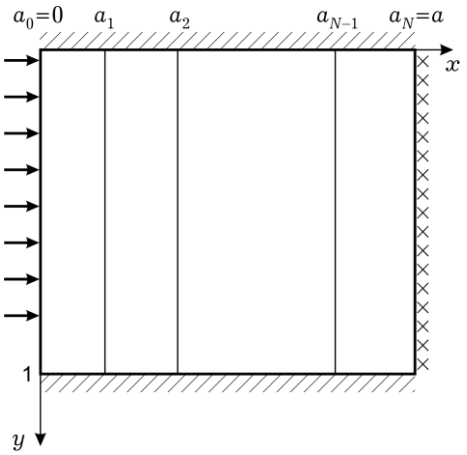

Fig. 1. Geometry and coordinate system of the problem.

Side $x = 0$, $0 < y < 1$ is loaded by the mechanical and the external pressure loads

$$\sigma_x^1\big|_{x=0} = -L(y) - \alpha_1 P(y), \qquad \tau_{xy}^1\big|_{x=0} = T(y), \qquad p_1\big|_{x=0} = P(y), \tag{1}$$

where $\sigma_x^\ell(x,y)$ and $\tau_{xy}^\ell(x,y)$ are dimensionless normal and tangential effective stress, respectively, $p_\ell(x,y)$ is the dimensionless pore pressure, α_ℓ are Biot's coefficients [12], $\ell = 1,\ldots,N$.

Bottom, $y = 0$, and top, $y = 1$, boundaries are assumed to be under the conditions of the perfect contact and impermeability:

$$\begin{aligned} &v_\ell\big|_{y=0} = 0, \qquad \tau_{xy}^\ell\big|_{y=0} = 0, \qquad \left.\frac{\partial p_\ell}{\partial y}\right|_{y=0} = 0, \\ &v_\ell\big|_{y=1} = 0, \qquad \tau_{xy}^\ell\big|_{y=1} = 0, \qquad \left.\frac{\partial p_\ell}{\partial y}\right|_{y=1} = 0, \qquad \ell = 1,\ldots,N. \end{aligned} \tag{2}$$

Here, $u_\ell(x,y)$ and $v_\ell(x,y)$ are dimensionless displacements of the solid skeleton, $\ell = 1,\ldots,N$.

Side $x = a$ is assumed to be rigidly fixed, i.e.

$$u_N\big|_{x=a} = 0, \qquad v_N\big|_{x=a} = 0, \tag{3}$$

while being either permeable

$$p_N\big|_{x=a} = 0 \tag{4}$$

or impermeable

$$\left.\frac{\partial p_N}{\partial x}\right|_{x=a} = 0. \tag{5}$$

The system of equilibrium and storage equations has the following form [25, p. 71, 72]:

$$\begin{aligned} &\frac{\partial^2 u_\ell}{\partial x^2} + \frac{\varkappa_\ell - 1}{\varkappa_\ell + 1}\frac{\partial^2 u_\ell}{\partial y^2} + \frac{2}{\varkappa_\ell + 1}\frac{\partial^2 v_\ell}{\partial x \partial y} - \alpha_\ell \frac{\varkappa_\ell - 1}{\varkappa_\ell + 1}\frac{\partial p_\ell}{\partial x} = 0, \\ &\frac{\partial^2 v_\ell}{\partial x^2} + \frac{\varkappa_\ell + 1}{\varkappa_\ell - 1}\frac{\partial^2 v_\ell}{\partial y^2} + \frac{2}{\varkappa_\ell - 1}\frac{\partial^2 u_\ell}{\partial x \partial y} - \alpha_\ell \frac{\partial p_\ell}{\partial y} = 0, \\ &\frac{\partial^2 p_\ell}{\partial x^2} + \frac{\partial^2 p_\ell}{\partial y^2} - \frac{\alpha_\ell}{K_\ell}\left(\frac{\partial u_\ell}{\partial x} + \frac{\partial v_\ell}{\partial y}\right) - \frac{S_{P,\ell}}{K_\ell} p_\ell = 0, \qquad \ell = 1,\ldots,N. \end{aligned} \tag{6}$$

Here, $\varkappa_\ell = 3 - 4\mu_\ell$ are Muskhelishvili's constants, μ_ℓ are the Poisson ratios, K_ℓ and $S_{P,\ell}$ are dimensionless values of $S_{p,\ell}$ and k_ℓ, $S_{p,\ell}$ are storativities of the pore space, k_ℓ are the permeability coefficients of ℓ-th layer.

The perfect contact is imposed on the layer interfaces [14]:

$$u_\ell\big|_{x=a_\ell-0} = u_{\ell+1}\big|_{x=a_\ell+0}, \qquad v_\ell\big|_{x=a_\ell-0} = v_{\ell+1}\big|_{x=a_\ell+0},$$

$$p_\ell\big|_{x=a_\ell-0} = p_{\ell+1}\big|_{x=a_\ell+0},$$

$$\sigma_x^\ell\big|_{x=a_\ell-0} = \sigma_x^{\ell+1}\big|_{x=a_\ell+0}, \qquad \tau_{xy}^\ell\big|_{x=a_\ell-0} = \tau_{xy}^{\ell+1}\big|_{x=a_\ell+0},$$

$$k_\ell \frac{\partial p_\ell}{\partial x}\bigg|_{x=a_\ell-0} = k_{\ell+1}\frac{\partial p_{\ell+1}}{\partial x}\bigg|_{x=a_\ell+0}, \qquad \ell = 1,\ldots,N-1. \tag{7}$$

The displacements, pore pressure and stress in each layer that satisfy boundary value problems (1)–(6) with coupling conditions (7) should be found.

2. The exact solution to the problem. The original problems (1)–(7) are reduced to the one-dimensional problems through the use of the finite sine and cosine Fourier transforms with respect to variable y [28]:

$$\begin{bmatrix} u_{\ell,\beta}(x) \\ v_{\ell,\beta}(x) \\ p_{\ell,\beta}(x) \end{bmatrix} = \int_0^1 \begin{bmatrix} u_\ell(x,y) \\ v_\ell(x,y) \\ p_\ell(x,y) \end{bmatrix} \begin{bmatrix} \cos\beta y \\ \sin\beta y \\ \cos\beta y \end{bmatrix} dy, \qquad \beta = \beta_n = \pi n, \qquad n = 0,1,2,\ldots. \tag{8}$$

The obtained one-dimensional boundary value problems are written in the vector form, as follows:

$$\mathbf{L}_2\mathbf{y}_{\ell,\beta}(x) = 0, \qquad a_{\ell-1} < x < a_\ell,$$

$$\mathbf{A}_{0,\beta}\mathbf{y}'_{1,\beta}(0) + \mathbf{B}_{0,\beta}\mathbf{y}_{1,\beta}(0) = \mathbf{g}_\beta,$$

$$\mathbf{A}_{1,\beta}\mathbf{y}'_{N,\beta}(a) + \mathbf{B}_{1,\beta}\mathbf{y}_{N,\beta}(a) = \mathbf{0},$$

$$\mathbf{y}_{\ell,\beta}\big|_{x=a_\ell-0} = \mathbf{y}_{\ell+1,\beta}\big|_{x=a_\ell+0},$$

$$\left(\mathbf{S}_\ell\mathbf{y}'_{\ell,\beta} + \mathbf{T}_\ell\mathbf{y}_{\ell,\beta}\right)\Big|_{x=a_\ell-0} = \left(\mathbf{S}_{\ell+1}\mathbf{y}'_{\ell+1,\beta} + \mathbf{T}_{\ell+1}\mathbf{y}_{\ell+1,\beta}\right)\Big|_{x=a_\ell+0}, \tag{9}$$

where $\mathbf{L}_2$ is the differential operator of the second order, $\mathbf{y}_{\ell,\beta}(x)$ is the vector containing unknown displacements and pore pressure transforms, $\mathbf{A}_{i,\beta}$, $\mathbf{B}_{i,\beta}$, $i = 0,1$, $\mathbf{S}_\ell$, $\mathbf{T}_\ell$, $\ell = 1,\ldots,N$, are known 3×3-matrices and $\mathbf{g}_\beta$ is the known vector shown in ***Appendix A***.

The apparatus of matrix differential calculation [15] is used in order to construct the general solution to boundary value problems (9). Hence, the solution of the corresponding matrix equations is to be found as

$$\mathbf{L}_2\mathbf{Y}_{\ell,\beta}(x) = 0, \qquad a_{\ell-1} < x < a_\ell, \qquad \ell = 1,\ldots,N, \tag{10}$$

where $\mathbf{Y}_{\ell,\beta}(x)$ are the 3×3-matrices. These matrices are to be represented as suggested in [7], and then substituted into the equation (10). The equalities

$$\mathbf{L}_2 e^{\xi x}\mathbf{I} = \mathbf{M}_{\ell,\beta}(\xi)e^{\xi x}, \qquad \ell = 1,\ldots,N,$$

are derived, where

$$\mathbf{M}_{\ell,\beta}(\xi)=\begin{pmatrix} \xi^2-\dfrac{æ_\ell-1}{æ_\ell+1}\beta^2 & \dfrac{2\beta}{æ_\ell+1}\xi & -\alpha_\ell\dfrac{æ_\ell-1}{æ_\ell+1}\xi \\ -\dfrac{2\beta}{æ_\ell-1}\xi & \xi^2-\dfrac{æ_\ell+1}{æ_\ell-1}\beta^2 & \alpha_\ell\beta \\ -\dfrac{\alpha_\ell}{K_\ell}\xi & -\dfrac{\alpha_\ell\beta}{K_\ell} & \xi^2-\beta^2-\dfrac{S_{P,\ell}}{K_\ell} \end{pmatrix}.$$

According to [15], the solutions of the matrix homogenous equations are found by formulae

$$\mathbf{Y}_{\ell,\beta}(x)=\frac{1}{2\pi i}\oint\limits_{C_\ell} e^{\xi x}\mathbf{M}^{-1}_{\ell,\beta}(\xi)\,d\xi,$$

where $\mathbf{M}^{-1}_{\ell,\beta}(\xi)$ are matrices inverse to the corresponding matrices $\mathbf{M}_{\ell,\beta}(\xi)$, $\ell=1,\ldots,N$. Closed contours C_ℓ cover all singularity points of the corresponding matrices $\mathbf{M}^{-1}_{\ell,\beta}(\xi)$, which are found exactly:

$$\xi=\pm\beta \qquad \text{and} \qquad \xi=\pm\sqrt{\beta^2+\frac{S_{P,\ell}}{K_\ell}+\frac{\alpha_\ell^2(æ_\ell-1)}{K_\ell(æ_\ell+1)}}\,.$$

Four fundamental matrix solutions $\mathbf{Y}_{\ell,i}(y)$, $i=1,\ldots,4$, $\ell=1,\ldots,N$, are constructed for each layer by using the residue theorem.

The vector solutions of the boundary value problems (9) are derived for the case where $\beta\neq 0$:

$$\mathbf{y}_{\ell,\beta}(x)=\big(\mathbf{Y}_{\ell,1}(x)+\mathbf{Y}_{\ell,3}(x)\big)\begin{pmatrix}c_{\ell,1}\\ c_{\ell,2}\\ c_{\ell,3}\end{pmatrix}+\big(\mathbf{Y}_{\ell,2}(x)+\mathbf{Y}_{\ell,4}(x)\big)\begin{pmatrix}c_{\ell,4}\\ c_{\ell,5}\\ c_{\ell,6}\end{pmatrix},$$
$$\ell=1,\ldots,N, \qquad (11)$$

where constants $c_{\ell,i}$, $i=1,\ldots,6$, should be determined from the boundary conditions and coupling conditions in (9). In order to find them the following matrices and vectors are introduced: 3×6-matrices

$$\mathbf{\Upsilon}_\ell(x)=\big(\mathbf{Y}_{\ell,1}(x)+\mathbf{Y}_{\ell,3}(x),\ \mathbf{Y}_{\ell,2}(x)+\mathbf{Y}_{\ell,4}(x)\big),$$

vectors of constants $\mathbf{C}_\ell=(c_{\ell,1},c_{\ell,2},c_{\ell,3},c_{\ell,4},c_{\ell,5},c_{\ell,6})^\top$, and square 6×6-matrices

$$\mathbf{H}_\ell(x)=\begin{pmatrix}\mathbf{\Upsilon}_\ell(x)\\ \mathbf{S}_\ell\mathbf{\Upsilon}'_\ell(x)+\mathbf{T}_\ell\mathbf{\Upsilon}_\ell(x)\end{pmatrix}.$$

Then using the form of general solution (11), the coupling conditions in (9) can be written as

$$\mathbf{H}_\ell(a_\ell)\mathbf{C}_\ell=\mathbf{H}_{\ell+1}(a_\ell)\mathbf{C}_{\ell+1}, \qquad \ell=1,\ldots,N-1.$$

According to the method proposed in [7] for layered media, constants corresponding to each layer can be expressed via the constants of the first layer $\mathbf{C}_1$:

$$\mathbf{C}_\ell=\mathbf{R}_\ell\mathbf{C}_1=\mathbf{H}^{-1}_\ell(a_{\ell-1})\mathbf{H}_{\ell-1}(a_{\ell-1})\ldots\mathbf{H}^{-1}_2(a_1)\mathbf{H}_1(a_1)\mathbf{C}_1, \quad \ell=2,\ldots,N. \qquad (12)$$

Expression (12) can be substituted into the boundary conditions in (9). Then the following system is derived

$$\big(\mathbf{A}_{0,\beta}\mathbf{\Upsilon}'_1(0)+\mathbf{B}_{0,\beta}\mathbf{\Upsilon}_1(0)\big)\mathbf{C}_1=\mathbf{g}_\beta,$$

$$\big(\mathbf{A}_{1,\beta}\mathbf{\Upsilon}'_N(a)+\mathbf{B}_{1,\beta}\mathbf{\Upsilon}_N(a)\big)\mathbf{R}_N\mathbf{C}_1=\mathbf{0}. \qquad (13)$$

System (13) is uniquely solvable so that vector $\mathbf{C}_1$ is found. Using it along with relations (12), the constants can be calculated for each layer.

The subcase when $\beta = 0$ is considered separately by similar approach which leads to the solution of problem for 2×2-matrices (***Appendix B***).

The application of inverse Fourier transform (8) to solutions (11) with the substitution of constants found from (12), (13) completes the construction of the exact analytical solution to the original problem.

3. The subcase of the problem for a multilayered semi-strip. The proposed approach can be extended towards the boundary value problem for a poroelastic multilayered semi-strip $0 < x < a$, $0 < y < \infty$ (see Fig. 2).

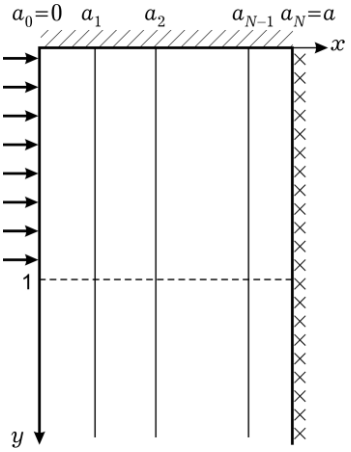

Fig. 2. Geometry and coordinate system of the poroelastic multilayered semi-strip.

The formulation of the latter problem repeats the formulation of the problem for a rectangular domain (1)–(7), taking into account the decrease in the sought displacement functions and the pore pressure at infinity.

The problems (1)–(7) are reduced to the one-dimensional boundary value problems by using semi-infinite sine and cosine Fourier transforms [24]:

$$\begin{bmatrix} u_{\ell,\beta}(x) \\ v_{\ell,\beta}(x) \\ p_{\ell,\beta}(x) \end{bmatrix} = \int_0^\infty \begin{bmatrix} u_\ell(x,y) \\ v_\ell(x,y) \\ p_\ell(x,y) \end{bmatrix} \begin{bmatrix} \cos\beta y \\ \sin\beta y \\ \cos\beta y \end{bmatrix} dy, \qquad \ell = 1,\ldots,N.$$

The successive solving in this subcase repeats the solving of the problem for a rectangular domain, taking into account the application of the inverse semi-infinite transform.

4. The numerical results and discussion. The derived analytical formulae allow for studying the poroelastic stress state of the multilayered rectangle and the semi-strip. The poroelastic properties of materials of layers are presented in Table 1.

Table 1. The characteristics of poroelastic materials [14].

Properties / Material	$G \times 10^{-9}$ [N/m^2]	μ	α	$k \times 10^{13}$ [m^4/(N × s)]	$S_p \times 10^{13}$ [m^2/N]
Ruhr sandstone	13.3	0.12	0.637	2.0	260.4
Ohio sandstone	6.8	0.181	0.729	56.0	1414.0
Boise sandstone	4.2	0.15	0.853	8.0	2.075

Two-layered and three-layered rectangular domains with equidistant layers are investigated under given loads. For the two-layered domains, the materials are chosen as *Boise sandstone* for $0 < x < a_1$ and *Ohio sandstone* for $a_1 < x < a$. For the three-layered domains the materials are chosen as *Ohio sandstone* for $0 < x < a_1$, *Ruhr sandstone* for $a_1 < x < a_2$, and *Boise sandstone* for $a_2 < x < a$.

The calculations are done for two types of external loads applied for the boundary $x = 0$:

- distributed normal mechanical load $L(y) = \sin(\pi y)$, $T(y) = 0$, $P(y) = 0$;
- distributed external pressure load $L(y) = 0$, $T(y) = 0$, $P(y) = 1$.

At all figures, the stress and pore pressures in the case when side $x = a$ is permeable are shown by solid lines while they are shown by dashed lines for the case when side $x = a$ is impermeable.

4.1. The numerical results for a rectangular poroelastic domain. The stress and pore pressures in the two-layered rectangle are shown in Fig. 3 and Fig. 4. The subcase of the distributed normal mechanical load is presented in Fig. 3. As it can be seen, the symmetry about the line $y = 1/2$ is observed, since the boundary conditions on the edges $y = 0$, $y = 1$ are the same, and the loading is symmetric. The tangential stress is determined only near the loaded boundary $x = 0$. The values of normal stress and pore pressure are higher when the boundary $x = a$ is impermeable.

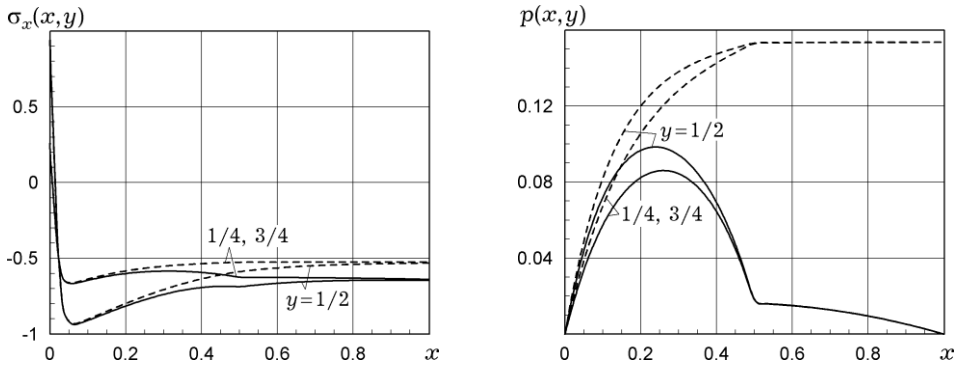

a) ***b***)

Fig. 3. The distribution of normal stress and pore pressure inside the two-layered rectangle for a distributed normal mechanical load.

The behavior of normal stress and pore pressure in the subcase of the distributed external pressure load is demonstrated in Fig. 4. The analyses of numerical results show that absolute values of normal stress and pore pressure are higher than in the previous subcase of load. The other tendencies also take place, i.e. the symmetry about line $y = 1/2$ and predominance of values for an impermeable boundary $x = a$.

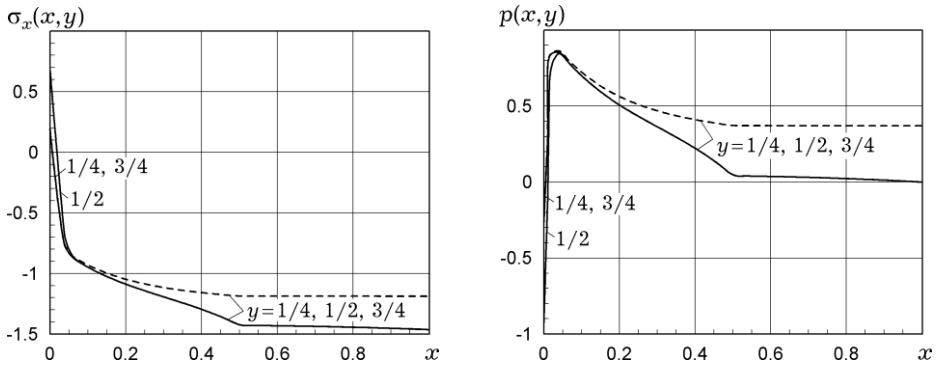

a) ***b***)

Fig. 4. The distribution of normal stress and pore pressure inside the two-layered rectangle for a distributed external pressure load.

In Fig. 5 and Fig. 6, the mechanical characteristics of the three-layered rectangular domain are presented. The middle layer has the smaller value of

Biot's coefficient than adjoining layers (see Table 1), so the values of the pore pressure for the subcase of the applied distributed normal mechanical load (see Fig. 5) are the highest for this layer. The general tendency is similar to the subcase of the two-layered rectangle.

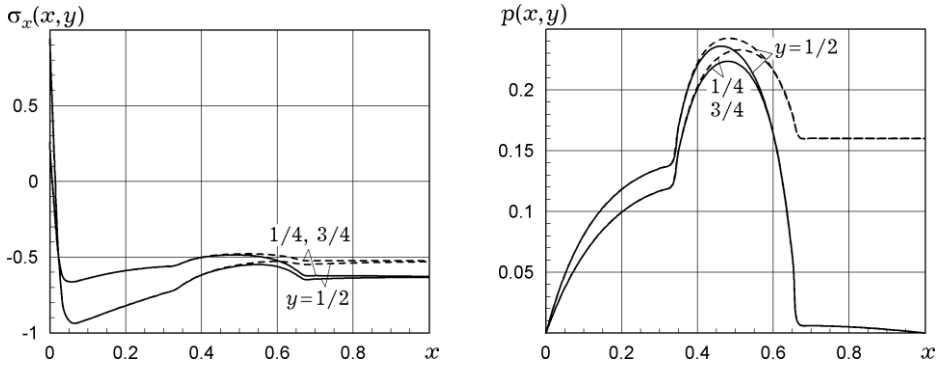

a) ***b***)

Fig. 5. The distribution of normal stress and pore pressure inside the three-layered rectangle for a distributed normal mechanical load.

As in the previous case, the absolute values of the normal stress and the pore pressure are analyzed in the subcase of the distributed external pressure load (Fig. 6). Evidently, the second layer with the smallest Biot's coefficient now exhibits a pronounced nonlinear pattern. The behavior of mechanical characteristics are quite similar to the previous subcase.

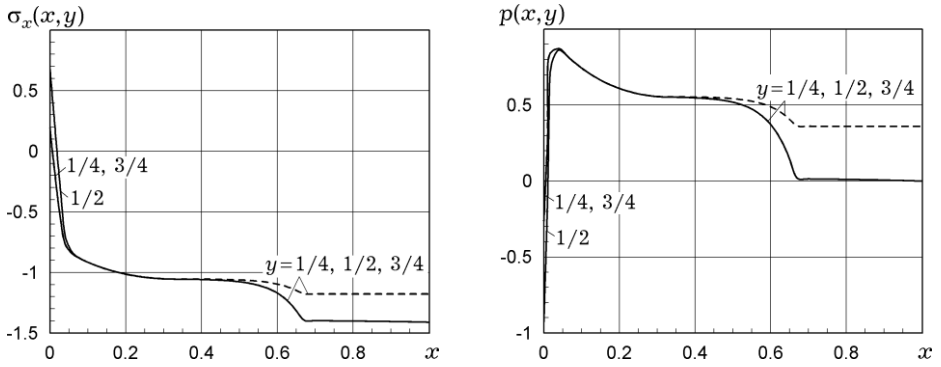

a) ***b***)

Fig. 6. The distribution of normal stress and pore pressure inside the three-layered rectangle regarding the change of poroelastic material for a distributed external pressure load.

4.2. The numerical results for a semi-strip. Similar numerical studies of the stress state of a poroelastic layered semi-strip for two types of loads are carried out for the cases of two- and three-layer structures. A significant difference in the behavior of mechanical characteristics is the lack of symmetry in their distribution, as well as lower absolute values of mechanical characteristics.

For a two-layer semi-strip, similarly to the case of a two-layer rectangular domain, the distribution of characteristics has a similar tendency. The nonlinear nature of the behavior of stress and pore pressure in the case of a three-layer semi-strip is revealed in the numerical analysis. Thus, in Fig. 7, it is noticeable that the pore pressure reaches its peak on the inner middle layer, after which the decrement in the values is observed. As in the case of a rectangular domain, the maximum pore pressure values are recorded for a

distributed pressure load (Fig. 8), while the maximum values of normal stress are observed under a distributed normal mechanical load.

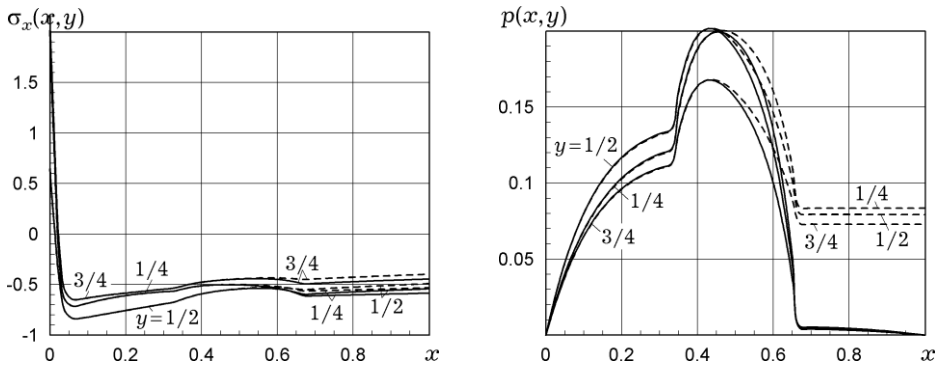

a) ***b***)

Fig. 7. The distribution of normal stress and pore pressure inside the three-layered semi-strip for a distributed normal mechanical load.

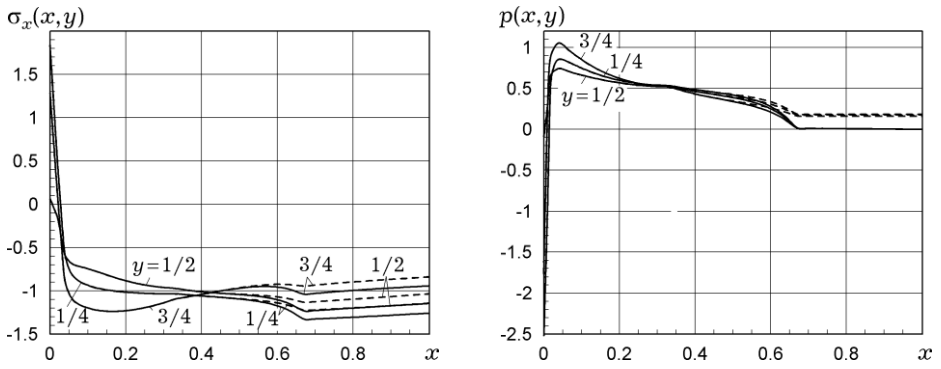

a) ***b***)

Fig. 8. The distribution of normal stress and pore pressure inside the three-layered semi-strip for a distributed external pressure load.

Conclusions. The analytical approach presented in the paper made it possible to derive the exact solutions of poroelastic problems for a multilayered rectangle and a semi-strip. Numerical calculations are provided for the two- and three-layered rectangle and semi-strip, and two cases of permeability of the right lateral boundary are considered for two different types of load.

The analysis of normal stress and pore pressure inside two- and three-layered poroelastic rectangular domains shows that the largest absolute values of normal stress and pore pressure are observed in the subcase of the distributed external pressure load applied to the left lateral side of the domain. The permeability of the right lateral boundary free from a load has substantial impact on the pore pressure and normal stress values inside the domain. These values are higher when this boundary is impermeable. Different poroelastic constants of layers play significant role in the distribution of pore pressure and normal stress, which can be seen in the figures for both two-layered and three-layered domains. The provided approach can be used for investigation of nonperfect contact conditions between the layers.

Acknowledgments. The research is supported by European project funded by Horizon 2020 Framework Programme for Research and Innovation (2014-2020) (H2020-MSCA-RISE-2020) Grant Agreement number 101008140 EffectFact "Effective Factorisation techniques for matrix-functions: Developing theory, numerical methods and impactful applications"; N. Vaysfeld acknowledges support from Royal Society Wolfson Visiting Fellowship R3/233003.

***Appendix A. The forms of matrices and vectors in vector boundary value problem* (9).**

The matrices and vectors shown in (9) have the following form:

$$\mathbf{L}_2\mathbf{y}_{\ell,\beta}(x) = \mathbf{I}\mathbf{y}''_{\ell,\beta}(x) - \mathbf{Q}_{\ell,\beta}\mathbf{y}'_{\ell,\beta}(x) - \mathbf{P}_{\ell,\beta}\mathbf{y}_{\ell,\beta}(x),$$

$\mathbf{I}$ is unit matrix,

$$\mathbf{y}_{\ell,\beta}(x) = \begin{pmatrix} u_{\ell,\beta}(x) \\ v_{\ell,\beta}(x) \\ p_{\ell,\beta}(x) \end{pmatrix}, \qquad \mathbf{Q}_{\ell,\beta} = \begin{pmatrix} 0 & -\dfrac{2\beta}{æ_\ell + 1} & \alpha_\ell \dfrac{æ_\ell - 1}{æ_\ell + 1} \\ \dfrac{2\beta}{æ_\ell - 1} & 0 & 0 \\ \dfrac{\alpha_\ell}{K_\ell} & 0 & 0 \end{pmatrix},$$

$$\mathbf{P}_{\ell,\beta} = \begin{pmatrix} \beta^2 \dfrac{æ_\ell - 1}{æ_\ell + 1} & 0 & 0 \\ 0 & \beta^2 \dfrac{æ_\ell + 1}{æ_\ell - 1} & -\alpha_\ell\beta \\ 0 & \dfrac{\alpha_\ell\beta}{K_\ell} & \beta^2 + \dfrac{S_{P,\ell}}{K_\ell} \end{pmatrix},$$

$$\mathbf{A}_{0,\beta} = \begin{pmatrix} 1-\mu_1 & 0 & 0 \\ 0 & 1 & 0 \\ 0 & 0 & 0 \end{pmatrix}, \qquad \mathbf{B}_{0,\beta} = \begin{pmatrix} 0 & \beta\mu_1 & 0 \\ -\beta & 0 & 0 \\ 0 & 0 & 1 \end{pmatrix},$$

$$\mathbf{g}_\beta = \begin{pmatrix} (1-2\mu_1)(\alpha_1 P_\beta - L_\beta)/2 \\ T_\beta \\ P_\beta \end{pmatrix},$$

$$\mathbf{S}_\ell = \begin{pmatrix} \dfrac{æ_\ell + 1}{æ_\ell - 1} G_\ell & 0 & 0 \\ 0 & G_\ell & 0 \\ 0 & 0 & k_\ell \end{pmatrix}, \qquad \mathbf{T}_\ell = \begin{pmatrix} 0 & \beta \dfrac{3 - æ_\ell}{æ_\ell - 1} G_\ell & 0 \\ -\beta G_\ell & 0 & 0 \\ 0 & 0 & 0 \end{pmatrix}.$$

The matrices $\mathbf{A}_{1,\beta}$, $\mathbf{B}_{1,\beta}$ take the form

$$\mathbf{A}_{1,\beta} = \begin{pmatrix} 0 & 0 & 0 \\ 0 & 0 & 0 \\ 0 & 0 & 0 \end{pmatrix}, \qquad \mathbf{B}_{1,\beta} = \begin{pmatrix} 1 & 0 & 0 \\ 0 & 1 & 0 \\ 0 & 0 & 1 \end{pmatrix}$$

for the permeable boundary condition (4), and

$$\mathbf{A}_{1,\beta} = \begin{pmatrix} 0 & 0 & 0 \\ 0 & 0 & 0 \\ 0 & 0 & 1 \end{pmatrix}, \qquad \mathbf{B}_{1,\beta} = \begin{pmatrix} 1 & 0 & 0 \\ 0 & 1 & 0 \\ 0 & 0 & 0 \end{pmatrix}$$

for the impermeable boundary condition (5).

***Appendix B. The subcase of the vector boundary value problem* (9) *when* $\beta = 0$.**

The boundary value problem (9) in the case $\beta = 0$ takes the following form:

$$\tilde{\mathbf{L}}_2\mathbf{y}_{\ell,0}(x) = \mathbf{0}, \qquad a_{\ell-1} < x < a_\ell,$$

$$\mathbf{A}_{0,0}\mathbf{y}'_{1,0}(0) + \mathbf{B}_{0,0}\mathbf{y}_{1,0}(0) = \mathbf{g}_0, \qquad \mathbf{A}_{1,0}\mathbf{y}'_{N,0}(a) + \mathbf{B}_{1,0}\mathbf{y}_{N,0}(a) = \mathbf{0},$$

$$\mathbf{y}_{\ell,0}\big|_{x=a_\ell-0} = \mathbf{y}_{\ell+1,0}\big|_{x=a_\ell+0}, \qquad (\mathbf{S}_{\ell,0}\mathbf{y}'_{\ell,0})\big|_{x=a_\ell-0} = (\mathbf{S}_{\ell+1,0}\mathbf{y}'_{\ell+1,0})\big|_{x=a_\ell+0},$$

(B.1)

where

$$\tilde{\mathbf{L}}_2\mathbf{y}_{\ell,0}(x) = \mathbf{I}\mathbf{y}''_{\ell,0}(x) - \mathbf{Q}_{\ell,0}\mathbf{y}'_{\ell,0}(x) - P_{\ell,0}\mathbf{y}_{\ell,0}(x),$$

$\mathbf{I}$ is unit matrix,

$$\mathbf{y}_{\ell,0}(x) = \begin{pmatrix} u_{\ell,0}(x) \\ p_{\ell,0}(x) \end{pmatrix}, \qquad \mathbf{Q}_{\ell,0} = \begin{pmatrix} 0 & \alpha_\ell \dfrac{æ_\ell - 1}{æ_\ell + 1} \\ \dfrac{\alpha_\ell}{K_\ell} & 0 \end{pmatrix}, \qquad \mathbf{P}_{\ell,0} = \begin{pmatrix} 0 & 0 \\ 0 & \dfrac{S_{P,\ell}}{K_\ell} \end{pmatrix},$$

$$\mathbf{A}_{0,0} = \begin{pmatrix} 1-\mu_1 & 0 \\ 0 & 0 \end{pmatrix}, \qquad \mathbf{B}_{0,0} = \begin{pmatrix} 0 & 0 \\ 0 & 1 \end{pmatrix}, \qquad \mathbf{S}_{\ell,0} = \begin{pmatrix} \dfrac{æ_\ell + 1}{æ_\ell - 1} G_\ell & 0 \\ 0 & k_\ell \end{pmatrix}.$$

The matrices $\mathbf{A}_{1,\beta}$, $\mathbf{B}_{1,\beta}$ take the form

$$\mathbf{A}_{1,0} = \begin{pmatrix} 0 & 0 \\ 0 & 0 \end{pmatrix}, \qquad \mathbf{B}_{1,0} = \begin{pmatrix} 1 & 0 \\ 0 & 1 \end{pmatrix}$$

for the permeable boundary conditions (4), and

$$\mathbf{A}_{1,0} = \begin{pmatrix} 0 & 0 \\ 0 & 1 \end{pmatrix}, \qquad \mathbf{B}_{1,0} = \begin{pmatrix} 1 & 0 \\ 0 & 0 \end{pmatrix}$$

for the impermeable boundary conditions (5).

The corresponding matrix equation $\tilde{\mathbf{L}}_2\mathbf{Y}_{\ell,0}(x) = \quad = 0$, $a_{\ell-1} < x < a_\ell$, $\ell = 1,\dots,N$, is considered. Its solution is found by the following formulae:

$$\mathbf{Y}_{\ell,0}(x) = \frac{1}{2\pi i} \oint_{\tilde{C}_\ell} e^{\xi x} \mathbf{M}^{-1}_{\ell,0}(\xi)\, d\xi,$$

where $\mathbf{M}^{-1}_{\ell,0}(\xi)$ are inverse matrices to the corresponding matrices

$$\mathbf{M}_{\ell,0}(\xi) = \begin{pmatrix} \xi^2 & -\alpha_\ell \dfrac{æ_\ell - 1}{æ_\ell + 1}\xi \\ -\dfrac{\alpha_\ell}{K_\ell}\xi & \xi^2 - \dfrac{S_{P,\ell}}{K_\ell} \end{pmatrix}, \qquad \ell = 1,\dots,N.$$

The closed contours $\tilde{C}_\ell$ cover all singularity points of the corresponding matrices $\mathbf{M}^{-1}_{\ell,0}(\xi)$, which are $\xi = 0$ and $\xi = \pm\sqrt{\beta^2 + \dfrac{S_{P,\ell}}{K_\ell} + \dfrac{\alpha_\ell^2(æ_\ell - 1)}{K_\ell(æ_\ell + 1)}}$. Using the residue theorem the system of three fundamental matrix solutions $\tilde{\mathbf{Y}}_{\ell,i}(y)$, $i = 1,2,3$, $\ell = 1,\dots,N$, is constructed.

The solution of the boundary value problem **(B.1)** which corresponds to the case when $\beta = 0$ has the following form:

$$\mathbf{y}_{\ell,0}(x) = (\tilde{\mathbf{Y}}_{\ell,1}(x) + \tilde{\mathbf{Y}}_{\ell,2}(x))\begin{pmatrix} \tilde{c}_{\ell,1} \\ \tilde{c}_{\ell,2} \end{pmatrix} + (\tilde{\mathbf{Y}}_{\ell,1}(x) + \tilde{\mathbf{Y}}_{\ell,3}(x))\begin{pmatrix} \tilde{c}_{\ell,3} \\ \tilde{c}_{\ell,4} \end{pmatrix},$$
$$\ell = 1,\dots,N, \qquad \textbf{(B.2)}$$

where constants $\tilde{c}_{\ell,i}$, $i=1,\dots,4$, should be found from the boundary conditions and coupling conditions in **(B.1)**. To find these constants, analogically to the general case, the following matrices and vectors are introduced: 2×4-matrices $\Upsilon_{\ell,0}=(\tilde{\mathbf{Y}}_{\ell,1}(x)+\tilde{\mathbf{Y}}_{\ell,3}(x),\tilde{\mathbf{Y}}_{\ell,1}(x)+\tilde{\mathbf{Y}}_{\ell,4}(x))$, vectors of constants $\tilde{\mathbf{C}}_{\ell,0}=(\tilde{c}_{\ell,1},\tilde{c}_{\ell,2},\tilde{c}_{\ell,3},\tilde{c}_{\ell,4})^{\top}$, and 4×4-matrices $\mathbf{H}_{\ell,0}(x)=\begin{pmatrix}\Upsilon_{\ell,0}(x)\\ \mathbf{S}_{\ell,0}\Upsilon'_{\ell,0}(x)\end{pmatrix}$. Then using the form of solution **(B.2)** the coupling conditions in **(B.1)** can be written as $\mathbf{H}_{\ell,0}(a_\ell)\tilde{\mathbf{C}}_{\ell,0}=\mathbf{H}_{\ell+1,0}(a_\ell)\tilde{\mathbf{C}}_{\ell+1,0}$, $\ell=1,\dots,N-1$. According to [7], constants corresponding to each layer can be expressed via the constants of the first layer $\tilde{\mathbf{C}}_{1,0}$:

$$\tilde{\mathbf{C}}_{\ell,0}=\mathbf{R}_{\ell,0}\tilde{\mathbf{C}}_{1,0}=\mathbf{H}^{-1}_{\ell,0}(a_{\ell-1})\mathbf{H}_{\ell-1,0}(a_{\ell-1})\dots\mathbf{H}^{-1}_{2,0}(a_1)H_{1,0}(a_1)\tilde{\mathbf{C}}_{1,0},$$
$$\ell=2,\dots,N. \qquad \textbf{(B.3)}$$

The expression **(B.3)** can be substituted into the boundary conditions in **(B.1)**. Then the following system is derived

$$(\mathbf{A}_{0,0}\Upsilon'_{1,0}(0)+\mathbf{B}_{0,0}\Upsilon_{1,0}(0))\tilde{\mathbf{C}}_{1,0}=\mathbf{g}_0,$$
$$(\mathbf{A}_{1,0}\Upsilon'_{N,0}(a)+\mathbf{B}_{1,0}\Upsilon_{N,0}(a))\mathbf{R}_{N,0}\tilde{\mathbf{C}}_{1,0}=\mathbf{0}. \qquad \textbf{(B.4)}$$

The system **(B.4)** is uniquely solvable, and vector $\tilde{\mathbf{C}}_{1,0}$ is found. Using it and relations **(B.3)** the constants of each layer are calculated.

1. *Гачкевич О. Р., Кушнір Р. М.* Вибрані проблеми механіки зв'язаних полів // Мат. методи та фіз.-мех. поля. – 2016. – **59,** № 1. – С. 7–24.
   Engl. translation: *Hachkevych O. R., Kushnir R. M.* Selected problems of the mechanics of coupled fields // J. Math. Sci. – 2018. – **229**, No. 2. – P. 115–132. – https://doi.org/10.1007/s10958-018-3666-7.
2. *Кіт Г. С., Івасько Н. М.* Двовимірна задача термопружності для півпростору з вільною, жорстко, гладко або гнучко закріпленою межею за теплоізоляції у паралельній до неї стрічковій області // Мат. методи та фіз.-мех. поля. – 2018. – **61,** № 2. – С. 80–90.
   Engl. translation: *Kit H. S., Ivas'ko N. M.* Two-dimensional problem of thermoelasticity for a half space whose boundary is either free or rigidly, smoothly, or flexibly fastened with heat insulation in a ribbon-like domain parallel to the boundary // J. Math. Sci. – 2021. – **253**, No. 1. – P. 84–98. – https://doi.org/10.1007/s10958-021-05215-7.
3. *Козачок О. П., Слободян Б. С., Мартиняк Р. М.* Взаємодія двох пружних тіл за наявності між ними періодично розташованих зазорів, заповнених реальним газом // Мат. методи та фіз.-мех. поля. – 2015. – **58,** № 1. – С. 103–111.
   Engl. translation: *Kozachok O. P., Slobodian B. S., Martynyak R. M.* Interaction of two elastic bodies in the presence of periodically located gaps filled with a real gas // J. Math. Sci. – 2017. – **222**, No. 2. – P. 131–142. – https://doi.org/10.1007/s10958-017-3287-6.
4. *Кубік Ю., Качмарик М., Чапля Є.* Про методи визначення характеристик пористих насичених середовищ // Фіз.-хім. механіка матеріалів. – 2001. – **37**, № 1. – С. 81–88.
   Engl. translation: *Kubik J., Kachmaryk M., Chaplya E.* Methods for the determination of the characteristics of porous saturated media // Mater. Sci. – 2001. – **37**, No. 1. – P. 92–102. – https://doi.org/10.1023/A:1012342523893.
5. *Кушнір Р. М., Махоркін І. М., Махоркін М. І.* Аналітично-числове визначення статичного термопружного стану плоских багатошарових термочутливих структур // Мат. методи та фіз.-мех. поля. – 2019. – **62,** № 4. – С. 131–140.
   Engl. translation: *Kushnir R. M., Makhorkin I. M., Makhorkin M. I.* Numerical-analytic determination of the static thermoelastic state of plane multilayer

thermosensitive structures // J. Math. Sci. – 2022. – **265**, No. 3. – P. 498–511. – https://doi.org/10.1007/s10958-022-06067-5.
6. *Михаськів В. М., Жбадинський І. Я., Степанюк О. І.* Використання потенціалів Гельмгольца для опису хвильового поля від динамічного розкриття множинних тріщин у біматеріалі // Мат. методи та фіз.-мех. поля. – 2007. – **50,** № 3. – С. 154–159.
7. *Попов Г. Я.* Точные решения некоторых краевых задач механики деформируемого твёрдого тела. – Одесса: Астропринт, 2013. – 421 с.
8. *Саврук М. П.* Двумерные задачи упругости для тел с трещинами. – Киев: Наук. думка, 1981. – 324 с.
9. *Ai Zh. Y., Gu G. L.* Dynamic behaviour of layered transversely isotropic poroelastic media subjected to rectangular harmonic loads // Int. J. Numer. Anal. Methods Geomech. – 2022. – **46**, No. 10. – P. 1941–1955. – https://doi.org/10.1002/nag.3375.
10. *Ai Zh. Y., Gu G. L., Zhao Y. Zh., Yang J. J.* An exact solution to layered transversely isotropic poroelastic media under vertical rectangular moving loads // Comput. Geotechn. – 2021. – **138**. – Article 104314. – https://doi.org/10.1016/j.compgeo.2021.104314.
11. *Ai Zh. Y., Hu Y. D., Cheng Y. Ch.* Non-axisymmetric consolidation of poroelastic multilayered materials with anisotropic permeability and compressible constituents // Appl. Math. Model. – 2014. – **38**, No. 2. – P. 576–587. – https://doi.org/10.1016/j.apm.2013.06.014.
12. *Biot M. A.* General theory of three-dimensional consolidation // J. Appl. Phys. – 1941. – **12**, No. 2. – P. 155–164. – https://doi.org/10.1063/1.1712886.
13. *Chen Y., Wang W., Ding Sh., Wang X., Chen Q., Li X.* A multi-layered poroelastic slab model under cyclic loading for a single osteon // BioMed. Eng. OnLine. – 2018. – **17**. – Article 97. – https://doi.org/10.1186/s12938-018-0528-y.
14. *Cheng A. H.-D.* Poroelasticity. – Ser.: Theory and Applications of Transport in Porous Media. – Vol. 27. – Cham: Springer, 2016. – xxvi+877 p. – https://doi.org/10.1007/978-3-319-25202-5.
15. *Gantmacher F. R.* The theory of matrices. – New York: Chelsea Publ. Co., 1959. – Vol. 1: x+377 p.; Vol. 2: x+277 p.
16. *Liu K., Zhang Zh., Pan E.* Dynamic response of a transversely isotropic and multilayered poroelastic medium subjected to a moving load // Soil Dynam. Earthq. Eng. – 2022. – **155**. – Article 107154. – https://doi.org/10.1016/j.soildyn.2022.107154.
17. *Nahirnyj T., Tchervinka K.* Mathematical modeling of the coupled processes in nanoporous bodies // Acta Mech. Automat. – 2018. – **12**, No. 3. – P. 196–203. – https://doi.org/10.2478/ama-2018-0030.
18. *Senjuntichai T., Kaewjuea W.* Dynamic response of multiple flexible strips on a multilayered poroelastic half-plane // J. Mech. Mater. Struct. – 2008. – **3**, No. 10. – P. 1885–1901. – https://doi.org/10.2140/jomms.2008.3.1885.
19. *Senjuntichai T., Keawsawasvong S., Rajapakse R. K. N. D.* Vertical vibration of multiple flexible strip foundations on multilayered transversely isotropic poroelastic soils // Int. J. Geomech. – 2021. – **21**, No. 11. – https://doi.org/10.1061/(ASCE)GM.1943-5622.0002210.
20. *Senjuntichai T., Phulsawat B., Keawsawasvong S., Kaewjuea W.* Dynamic impedances of multiple strips on multi-layered transversely isotropic poroelastic soils // Forces in Mechanics. – 2024. – **14**. – Article 100260. – https://doi.org/10.1016/j.finmec.2024.100260.
21. *Singh S. J., Rani S.* Plane strain deformation of a multi-layered poroelastic half-space by surface loads // J. Earth Syst. Sci. – 2006. – **115,** No. 6. – P. 685–694. – https://doi.org/10.1007/s12040-006-0001-3.
22. *Stache J. M.* Transient analysis of multilayered poroelastic flexible pavements // Int. Conf. on Transportation and Development (ICTD 2024, June 15–18, 2024. Atlanta, Georgia). – 2024. – https://doi.org/10.1061/9780784485538.007.
23. *Tokovyy Y. V.* Elastic and thermoelastic response of multilayer inhomogeneous hollow cylinders // Mech. Adv. Mater. Struct. – 2024. – **31**, No. 17. – P. 3889–3901. – https://doi.org/10.1080/15376494.2023.2186548.
24. *Vaysfeld N. D., Zhuravlova Z. Yu.* Response of a poroelastic semi-infinite strip to the compression acting upon its lateral sides // Мат. методи та фіз.-мех. поля. – 2022. – **65**, № 1-2. – P. 199–208.

***Engl. translation*:** *Vaysfeld N. D., Zhuravlova Z. Yu.* Response of a poroelastic semi-infinite strip to the compression acting upon its lateral sides // J. Math. Sci. – 2024. – **282**, No. 5. – P. 849–861. – https://doi.org/10.1007/s10958-024-07220-y.

25. *Verruijt A.* An introduction to soil dynamics. – Ser.: Theory and applications of transport in porous media. – Vol. 24. – Dordrecht, etc.: Springer, 2010. – xiv+433 p. – https://doi.org/10.1007/978-90-481-3441-0.
26. *Wang F., Ding T., Han X., Lv L.* Dynamic Green's functions for an anisotropic multilayered poroelastic half-space // Transport in Porous Media. – 2020. – 133, No. 2. – P. 293–312. – https://doi.org/10.1007/s11242-020-01424-x.
27. *Wang R., Kümpel H.-J.* Poroelasticity: Efficient modeling of strongly coupled, slow deformation processes in multilayered half-space // Geophysics. – 2003. – 68, No. 2. – P. 705–717. – https://doi.org/10.1190/1.1567241.
28. *Zhuravlova Z.* Exact solution of the plane problems for poroelastic rectangle and semi-strip // Z. Angew. Math. Mech. – 2022. – **102**, No. 11. – e202200162. – https://doi.org/10.1002/zamm.202200162.

ТОЧНИЙ РОЗВ'ЯЗОК ЗАДАЧІ ПОРОПРУЖНОСТІ ДЛЯ ШАРУВАТОЇ ПРЯМОКУТНОЇ ОБЛАСТІ

Розглядається поропружний напружений стан шаруватої прямокутної області в термінах крайової задачі теорії поропружності. Запропонований аналітичний метод розв'язання у випадку ідеального контакту між шарами дає змогу побудувати точний розв'язок задачі. Отримані у явному вигляді формули для визначення напружень, переміщень та тиску рідини відкрили можливість проведення всесторонніх числових досліджень, які демонструють залежність напруженого стану від поропружних властивостей матеріалів. Описаний підхід до розв'язання може бути розширено на випадок, коли між шарами задано умови «м'якого» чи «жорсткого» контактів.

Ключові слова: *поропружна шарувата прямокутна область, інтегральне перетворення, матричне диференціальне числення, точний розв'язок.*

Odesa I. I. Mechnikov National University, Odesa

Received 07.08.24